

The ScaRaB-Resurs Earth Radiation Budget Dataset and First Results



J.-Ph. Duvel,^{*} M. Viollier,⁺ P. Raberanto,⁺ R. Kandel,⁺ M. Haeffelin,[#]
L. A. Pakhomov,[@] V. A. Golovko,[&] J. Mueller,^{**++} R. Stuhlmann,^{**}
and the International ScaRaB Scientific Working Group

ABSTRACT

Measurements made by the second flight model of the Scanner for Radiation Budget (ScaRaB) instrument have been processed and are now available for the scientific community. Although this set of data is relatively short and sparse, it is of excellent quality and is the only global broadband scanner radiance information for the period between October 1998 and April 1999. This second flight model marks the conclusion of the ScaRaB cooperative program of France, Russia, and Germany. The two flight models of the ScaRaB instrument gave broadband radiance measurements comparable in quality to those made by the Earth Radiation Budget Experiment and the Clouds and Earth Radiant Energy System scanning instruments. In addition, the ScaRaB instrument gave unique results for the comparison between narrowband (visible and infrared atmospheric window) and broadband radiance measurements. These measurements were mostly used to improve the broadband data processing and to study the error budget resulting when narrowband channel data are used to estimate the earth radiation budget. These concomitant narrow- and broadband measurements made by the two flight models of ScaRaB contain original information of considerable interest for further scientific use.

1. Introduction

The second flight model of the Scanner for Radiation Budget (ScaRaB) instrument was integrated on the Russian satellite *Resurs 01-4* and launched on

10 July 1998 from the Baikonour (Kazakhstan) spaceport. The ScaRaB program was a cooperative program of France, Russia, and Germany that was also assisted by the International ScaRaB Scientific Working Group (see Table 1 in Kandel et al. 1998). The objective of this program was to make space measurements of the earth radiation budget in complement to those provided by the Earth Radiation Budget Experiment (ERBE) (Barkstrom et al. 1989) and the Clouds and Earth Radiant Energy System (CERES) missions (Wielicki et al. 1996). The first flight model of ScaRaB on the Russian operational weather satellite *Meteor-3/7* gave observations of the earth radiation fluxes from March 1994 to March 1995 (Kandel et al. 1998).

The earth radiation budget at the top of the atmosphere (TOA) is a key parameter that measures the energy exchange between the earth climate system and space. The TOA ERB may be estimated using broadband measurements from space of reflected solar or shortwave (SW: 0.2–4 μm) radiation and of outgoing infrared or longwave (LW: 4–100 μm) radiation (cf., e.g., Raschke et al. 1973; Stephens et al. 1981;

^{*}Laboratoire de Météorologie Dynamique, Ecole Normale Supérieure, Paris, France.

⁺Laboratoire de Météorologie Dynamique, Ecole Polytechnique, Palaiseau, France.

[#]Virginia Polytechnic Institute and State University, Blacksburg, Virginia.

[@]Research Center for Earth Operative Monitoring, Moscow, Russia.

[&]Scientific Research Center for Space Hydrometeorology, Moscow, Russia.

^{**}Institute for Atmospheric Physics, GKSS Research Center, Geesthacht, Germany.

⁺⁺Current affiliation: EUMETSAT, Darmstadt, Germany.

Corresponding author address: J. Ph. Duvel, LMD-ENS, 24, Rue Lhomond, 75231 Paris, Cedex 05, France.

E-mail: jpduvel@lmd.ens.fr

In final form 5 January 2001.

© 2001 American Meteorological Society

Jacobowitz et al. 1984; House et al. 1986; Hartmann et al. 1986; Kandel 1990). Such space measurements of regional radiation fluxes are required to document the origin and the variability of the distribution of radiative energy sources and sinks. In particular, the so-called cloud radiative forcing (CRF; Coakley and Baldwin 1984; Charlock and Ramanathan 1985; Ramanathan et al. 1989) is a very important parameter of the role of different types of cloud in the energy balance of the climate system. Changes in the CRF parameter accompanying perturbations of the atmospheric state give the sign and magnitude of cloud radiative feedback in climate variations. The CRF parameter must be correctly simulated by a general circulation model (GCM) of the present climate if that model is to be judged valid. This is a necessary although probably not sufficient condition for obtaining a correct estimate of the sensitivity of the climate system (cf., e.g., Cess et al. 1990). This is not straightforward since the CRF parameter integrates the results of many different processes (cloud generation, cloud microphysics, cloud geometry) that lead to varied cloud occurrence and radiative effect. In any event, both at the instantaneous and at the monthly mean timescale, broadband radiative fluxes at the TOA result from an integration of many surface and atmospheric processes. The necessary evaluation of the validity of the representation of cloud processes in GCMs must thus be a verification of a large spectrum of parameters, including the diurnal variation of cloud occurrence, which may profoundly influence the radiative effect in the SW and other effects incorporated in the CRF parameter. For these reasons, and also to detect and study variations of the clear-sky greenhouse effect (Raval and Ramanathan 1989), the broadband LW and SW radiances must be measured at a spatial scale of a few tens of kilometers, that is, the typical size of ERBE, ScaRaB, or CERES field of view.

Measured variations of the ERB may indicate changes in the climate system, but also require additional observations to define the precise nature and the reason of the change. On the one hand, various global radiation fluxes at the TOA may correspond to the same average temperature at the earth's surface; and on the other hand, different surface and atmospheric temperature distributions may yield the same TOA radiation fluxes. This is because of the complex action of cloudiness (Fouquart et al. 1990; Stephens and Greenwald 1991b) and of atmospheric composition and structure (Stephens and Greenwald 1991a; Bony

and Duvel 1994; Bony et al. 1995; Duvel et al. 1997) on the global greenhouse effect. The accuracy of these ERB measurements is also probably not sufficient to monitor eventual imbalance in the global fluxes resulting from slow warming or cooling of the global climate system (Stowe 1988; Wielicki et al. 1996). One may note, for example, that the estimated ocean warming since 1950 corresponds to a global mean flux (at the surface, not TOA) of order 0.3 W m^{-2} (Levitus et al. 2000). However, other large-scale parameters, such as the meridional distribution of zonal mean radiative fluxes, may certainly be monitored by ERB experiments, giving information on modulations or trends in the meridional energy transfer by the atmosphere and the ocean. It is thus important to have a continuous set of ERB measurements, not only to do such monitoring, but also to give more sampling of typical climate variations including strong El Niño or La Niña events or other large perturbations due for example to atypical monsoons or to volcanic eruptions. This point is especially important to test the sensitivity of GCMs in regard to a large spectrum of climate conditions. It is in this context that the ScaRaB program was initiated in 1986.

The ScaRaB program was designed to provide measurements of the broadband SW and LW fluxes with, as for ERBE and CERES, a spatial resolution adequate for the detection of clear scenes and thus for the determination of the CRF parameter. Two narrowband channels were also added to the ScaRaB scanning radiometer instrument in order to test the cloud/clear-sky detection (Briand et al. 1997). Various applications of these auxiliary narrowband channels have been described (Stubenrauch et al. 1993; Li and Trishchenko 1999; Duvel et al. 2000; Duvel and Raberanto 2000). The ScaRaB program also gave opportunities to fill the gap of scanner measurements between the end of operation of the ERBE scanner on the Earth Radiation Budget Satellite (ERBS) in 1989, and the beginning in 1997 of CERES measurements. The interest here was to sample the regional-scale interannual variability of broadband fluxes during the period of nearly 10 years otherwise without any broadband scanner measurements. After the relative success of the first flight model of ScaRaB on the *Meteor-3/7* with one year of data between March 1994 and March 1995, it was decided to launch the second flight model on a Resurs platform. Unfortunately, because of transmitter failures on the *Resurs 01-4* platforms, the data collected from this second flight model are relatively sparse, even in the period of measurement from

October 1998 to April 1999. However, the data collected are of excellent quality and are now available to the broader scientific community for further scientific use.

The aim of this article is to give an overview of the ScaRaB-Resurs experiment. Since the instrument and the data processing are very similar to those utilized for the ScaRaB-Meteor experiment (Kandel et al. 1998), only a summary is given in section 2. The emphasis is on the differences in the orbital configuration and in the calibration procedure. An overview of the measurements is given in section 3 and conclusions on the ScaRaB program in section 4.

2. The ScaRaB-Resurs experiment

a. The ScaRaB instrument

The ScaRaB instrument (Fig. 1) is a cross-track scanning radiometer with four channels. A precise description of the instrument may be found in Monge et al. (1991) and in Kandel et al. (1998). Each channel is a small telescope focusing the incoming radiation onto a pyroelectric detector placed at the prime focus of a spherical aluminium mirror. The four channels are mounted perpendicular to the axis of a rotor cylinder. The radiation arriving on each detector is chopped at the pixel sampling frequency. The two choppers are rotating hemispherical mirrors with two openings giv-

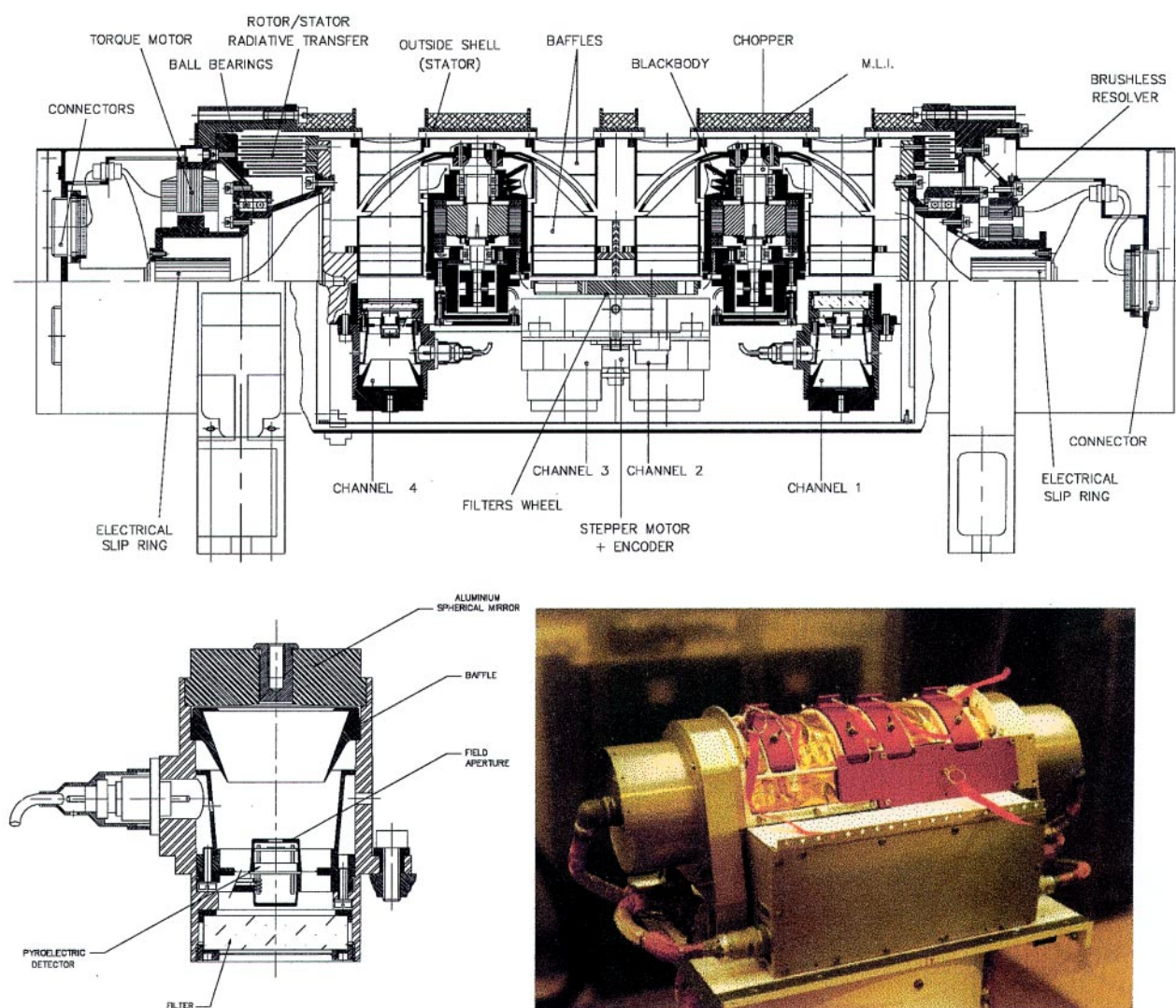


FIG. 1. (top) Optical head design with the four channels and the two choppers mounted on a scanning optical bench (rotor). Channels 1–4 are the VIS, SW, TW, and IRW channels, respectively. (bottom left) Channel design with the BARNES pyroelectric detector placed at the prime focus of a spherical aluminium mirror. (bottom right) Picture of the ScaRaB instrument with the Russian calibration block. The red parts are obstructions of earth and space views to protect the radiometers prior to launch. Note that only the VIS channel on the right has no real space view.

ing alternately the radiation coming from the outside and the radiation reflected from a small “reference” internal blackbody. A radiance measurement is given by the difference between the signal from the outside (earth view or calibration source) and the signal from the reference internal blackbody.

There are two broadband channels, the shortwave (SW: 0.2–4- μm) channel and the total radiation (TW: 0.2–100- μm) channel, from which the longwave (LW: 4–100 μm) is deduced. During nighttime, the LW radiance is directly given by the TW channel. During daylight, however, the LW radiance is given by a difference between the TW and the SW radiance measurements. Since the ScaRaB TW and SW channels have very similar spectral response in the shortwave spectral domain, no additional spectral correction is necessary to determine the LW radiance from such a difference. However, as for ERBE or CERES, an excellent cross-calibration between the SW and the TW channel is required. An interesting and original characteristic of the ScaRaB instrument is the presence of two additional narrowband channels in the visible (VIS: 0.55–0.65 μm) and in the infrared window (IRW: 10.5–12.5 μm). These narrowband channels are especially useful for precise assessment of the error resulting when narrow band data are used to estimate the earth radiation budget (Duvel et al. 2000). Also, the IRW channel may be used to compute or verify the cross-calibration between the SW and the TW channels (Duvel and Raberanto 2000) or to estimate angular correction for the determination of the LW flux from LW and IRW radiance measurements (Stubenrauch et al. 1993).

b. The ScaRaB-Resurs calibration procedure

The onboard calibration of the ScaRaB radiometers is nominally performed using a calibration module (Fig. 1) containing high quality blackbodies for the longwave part of the spectrum and lamps for the shortwave part. As for the first ScaRaB flight model, the scanner characterization and calibration of the onboard blackbody simulators were carried out in a vacuum chamber at the Institut d’Astrophysique Spatiale in Orsay, France. The calibration procedure described in Kandel et al. (1998) checks the linearity of the radiometer response and determines the emissivity of the onboard calibration blackbodies and the temperature dependence of detector gains. For each channel (c), the generic equation for the conversion between instrumental count (N_c) and the so-called filtered (i.e., by the spectral response of the radiometer) radiance is

$$N_c = G_c \left[\int_0^\infty L_{\text{SW}}(\lambda) r_c(\lambda) d\lambda + \int_0^\infty L_{\text{LW}}(\lambda) r_c(\lambda) d\lambda \right], \quad (1)$$

where G_c is the gain of the channel, r_c is its spectral response and L_{SW} and L_{LW} are, respectively, the SW radiance, and the LW radiance of the earth scene (i.e., respectively the reflected solar radiance or the emitted thermal radiance) or of the calibration sources.

The shortwave sources were calibrated using the solar Ground Calibration Unit operated (for ScaRaB-Resurs) at Odeillo in southwest France. This calibration procedure, described by Mueller et al. (1993, 1996, 1997), gives a verification of the spectral response of the radiometers by comparing the detector gains obtained on known infrared and solar sources. The accuracy of the ground calibration is estimated to be 0.4% for the onboard blackbodies and 1.5% for the onboard lamp sources. For the ScaRaB-Resurs instrument, additional calibrations were performed using an integrating sphere (Dinguirard et al. 1998).

In-flight operation modes include earth measurement and calibration modes. Each cycle of the earth measurement mode includes an earth scan of 102°, a space look, and a measurement on onboard blackbodies and lamps (turned on for certain cycles). Note that for ScaRaB Flight Model 2 on board sun-synchronous Resurs, true space looks is obtained also for the SW channel and not only for the TW and IRW channels as was the case for ScaRaB-Meteor. There are two principal calibration modes. The first one, activated every 12 h, improves the calibration of the radiometers by looking at blackbodies, lamps, and space during a longer period of time and by looking at lamps that are not observed during the earth measurement mode. The second calibration mode is activated once a month and measures the SW gain on less frequently used reference lamps. This mode was used with success for ScaRaB-Meteor to establish the in-flight relationship between the temperature of the instrument and the gain of the SW channel.

For ScaRaB-Resurs, only a few sets of measurements were taken using this second calibration mode. In addition, there were some discrepancies between the different ground calibration approaches tested for this second flight model (Dinguirard et al. 1998) making the application of the nominal calibration procedure difficult. For these reasons, the gain of the SW channel was deduced from a geophysical cross-calibration between the TW and the SW channels. This cross-calibration (Duvel and Raberanto 2000) is based on the estimate of the SW radiance of the TW channel

during daylight by removing the LW radiance estimated from the IRW channel. Obviously, because of the variability of the atmospheric absorption, it is not possible to find a precise and unique relation between the IRW and the LW radiances for all observations. However, as shown in Duvel and Raberanto (2000), it is possible to estimate the LW radiance with an accuracy better than $1 \text{ W m}^{-2} \text{ sr}^{-1}$ from the measurement of the IRW radiance over the tops of high and cold deep tropical (20°N – 20°S) convective clouds. In addition to the relatively small and homogeneous atmospheric absorption above, these clouds are also very bright and cold and give potentially a small LW radiance compared to the SW radiance. The error due to the estimate of the LW radiance from the IRW measurement is further minimized in regard to the large signal in the SW. The relation between the LW radiance and the IRW radiance for these specific scene types (defined by IRW blackbody temperature lower than 230 K in the latitudinal band 20°N – 20°S) is obtained using nighttime ScaRaB measurements. Once the LW part of the TW radiance of these clouds is removed during daylight, it is possible to compare directly the SW part of the well-calibrated TW radiance to the SW radiance and thus to adjust the SW channel gain. The geophysical calibration approach gives calibration of the SW channel and cross calibration with TW channel with accuracy better than 1%.

The in-flight calibration (i.e., determination of the gain) of the four channels of ScaRaB-Resurs is based on the linear relationship between the temperature of the instrument and the gain G_C [Eq. (1)] of each channel. For the LW and the IRW channels, the linear coefficients are obtained a posteriori from the numerous

in-flight blackbody measurements. For the SW channel, the linear relationship between the temperature of the instrument and the gain G_C is computed on the basis of daily values of the SW gain obtained from the geophysical cross-calibration approach. Finally, the gain of the VIS channel is obtained by considering that the ratio between the gain of the SW and the VIS channels (i.e., $G_{\text{SW}}/G_{\text{VIS}}$) stayed constant and equal to the ratio established during ground calibration. This calibration of the VIS channel of ScaRaB is believed to

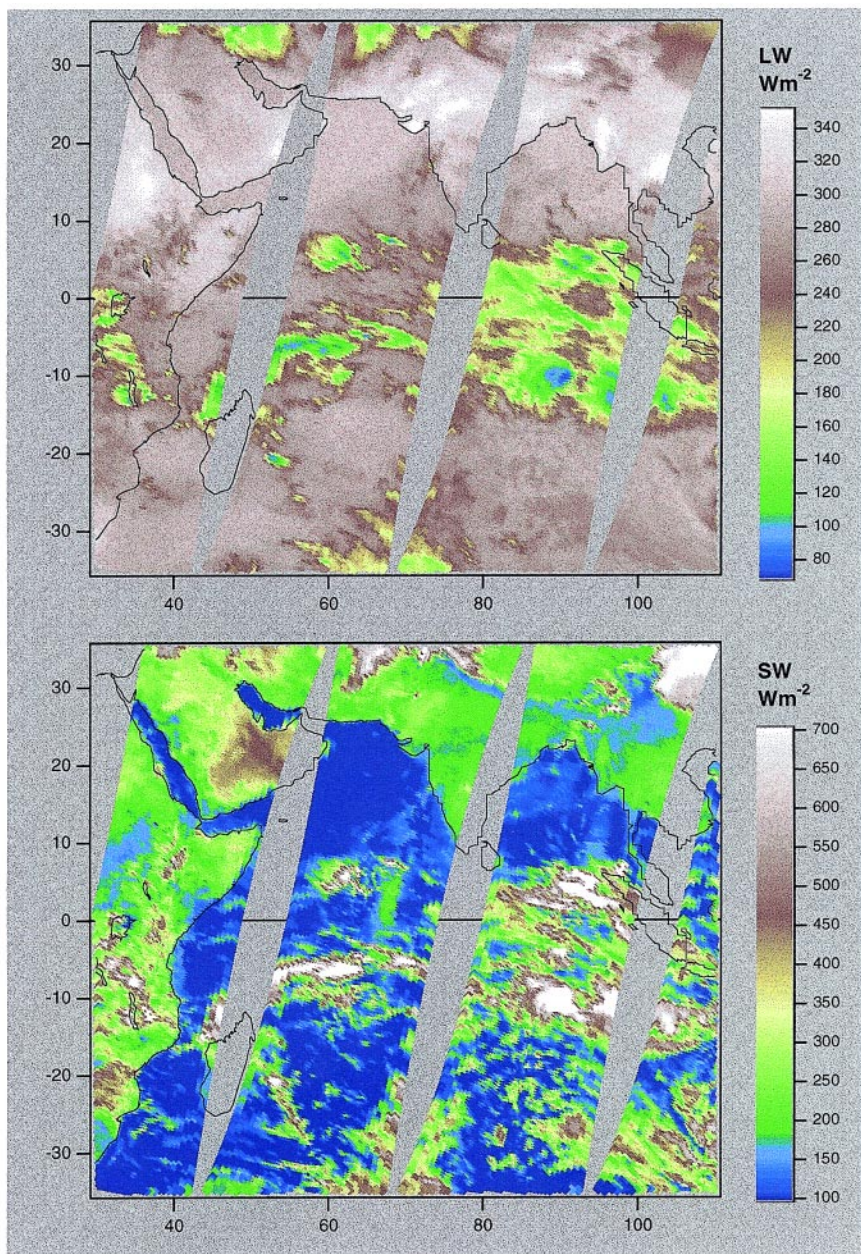


FIG. 2. Four daylight orbits of ScaRaB-Resurs on 19 Mar 1999 over the Indian Ocean region for (top) the LW fluxes and (bottom) the SW reflected fluxes at the pixel horizontal resolution.

be more reliable than the calibration obtained using the calibration source of the VIS channel (i.e., considering that the VIS channel radiance of the lamp stays constant).

c. Data processing

Resurs 01-4 is a sun synchronous satellite in polar orbit (inclination 98.8°), with perigee at 815 km and apogee at 818 km. The local time of equatorial crossing is around 2215 LST. This is a major change from the ScaRaB-Meteor, which had a polar orbit at 1200 km with an inclination of 82.5° and thus a precession of the orbit with a period of around 7 months. With the sun-synchronous orbit of Resurs, most of the variable bias in the products, due to changes in the local time of observation, is eliminated. With ScaRaB at lower altitude, the swath of each scan was smaller, giving gaps from one orbit to the next near the equator (Fig. 2). The field of view is defined by a square field stop with a diagonal parallel to the scan direction. For Resurs at 815-km altitude, the nadir projection on the ground of the instantaneous field of view is a 41-km square. The distance between two adjacent pixels is 29 km.

The data processing of ScaRaB is an ERBE-like processing (Viollier et al. 1995) that is only summarized here. The first step after the determination of the filtered SW and LW radiances [Eq. (1)] is to determine the scene type (i.e., cloud-cover estimate) using a maximum likelihood technique. Then a spectral correction is applied to deduce the SW radiance from the filtered SW radiance. This spectral correction is necessary in the SW because of the imperfect flatness of the spectral response. The next step is to apply scene-type-dependent angular correction models to deduce the SW and LW fluxes ($W m^{-2}$) of the pixel as a function of the measured radiances. These fluxes are averages over a geographical area of $2.5^\circ \times 2.5^\circ$ latitude and longitude. Diurnal models are then applied in order to compute regional monthly mean values of the mean and clear-sky fluxes.

The available data are summarized in Fig. 3. One can see that a large amount of data is missing. This poor data coverage is not due to a deficiency of the ScaRaB instrument but to the failure of a first platform



Fig. 3. Schematic of the data coverage of the ScaRaB-Resurs experiment.

transmitter due to a software problem. In order to avoid a premature failure of the second and last transmitter, it was necessary to send the remote command to the satellite manually twice a day instead of using the onboard software requiring only one remote command by day. The missing ScaRaB data are the result of the required adaptation of the Russian ground segment of the Resurs platform to this new configuration. The ScaRaB instrument was operating nominally during the entire mission and available satellite housekeeping data indicate that it was still functioning at the end of year 2000. Unfortunately, no scientific data were transmitted.

3. First analysis of ScaRaB-Resurs measurements

a. ScaRaB-CERES cross calibration

The availability of the ScaRaB-Resurs data at the same time as CERES-Tropical Rainfall Measurement Mission (TRMM) data gave an opportunity to cross-calibrate the two instruments. The CERES instrument was turned on during a few orbits during periods favorable for the comparison with ScaRaB-Resurs. The scanning azimuth of the CERES instrument was rotated so as to obtain parallel scans for the two instruments. This is necessary to compare precisely the SW radiances, which are very sensitive to the viewing and solar zenith angles and to the azimuth between the sun and the satellite. This cross-calibration exercise, described in Haeffelin et al. (2001) shows that the radiances in the SW domain are in agreement within

1.5% \pm 1% (95% confidence level) with ScaRaB radiances larger. The radiances in the LW domain are in agreement within 0.7 \pm 0.1% during day and 0.5% \pm 0.1% during night with CERES radiance larger.

In the SW domain, this good agreement demonstrates the consistency of the very different calibration and spectral correction procedures between the two instruments. In the LW domain, the good agreement for both daytime and nighttime radiance measurements confirms first the good absolute calibration of the LW part of both CERES and ScaRaB radiometers. In addition, the consistency between the LW daytime and nighttime comparisons demonstrates that the ScaRaB and CERES procedures to obtain the LW radiance from total and SW radiance measurements during daylight perform consistently. The comparisons also support the absolute character of the calibration of these two instruments for both the LW and SW spectral domains.

b. Analysis of monthly mean values

1) ERROR ANALYSIS

Due to the relatively sparse data coverage of ScaRaB-Resurs (Fig. 3), the monthly mean values have to be considered with care. The first step of this section is thus to estimate the error on monthly means resulting from this degraded time sampling, compared to the time sampling given by a polar orbiting platform. In fact, the ERBE-like processing of ScaRaB (Viollier et al. 1995) accounts for missing data in the computation of monthly averages. For example, in the LW domain, the fluxes are extrapolated and interpolated to all missing hours. There are then two approaches to compute the monthly means, one from the

TABLE 1. Differences between monthly daily regional means and monthly hourly regional means for the LW flux ($W m^{-2}$).

	Global means	Standard deviation	Tropical means
Nov 1998	0.4	4.5	0.1
Dec 1998	0.3	5.9	0.8
Jan 1999	-0.3	12.0	-0.7
Feb 1999	0.0	1.6	0.1
Mar 1999	0.0	2.5	0.1

TABLE 2. Differences in the LW fluxes ($W m^{-2}$) for ScaRaB-Meteor dataset processed with all measurements or with a time-sampling corresponding to the ScaRaB-Resurs measurements.

	Global means	Standard deviation	Tropical means
Nov 1994	-0.1	8.8	-0.4
Dec 1994	-0.5	7.0	-0.7
Jan 1995	-0.6	11.5	-0.5
Feb 1995	-0.1	2.7	-0.0
Mar 1994	0.0	3.0	-0.0

monthly daily regional means (MDM) that consider all the daily averaged fluxes, the other from the monthly hourly regional means (MHN), that is calculated considering only days with at least one LW measurement. The difference between the two products thus increases with the number of days without measurements. Differences between MDM and MHM for global and tropical (20°S, 20°N) LW fluxes, resulting from different weighting of the available measurements, are however less than 0.5 and 1 $W m^{-2}$, respectively (Table 1). For regional means, the standard deviation of differences is largest (12 $W m^{-2}$) for January but relatively small for February and March 1999.

Another way to estimate the ScaRaB-Resurs time-sampling error is to reprocess the existing well-sampled measurements of ScaRaB-Meteor for a particular month but with the reduced sampling of ScaRaB-Resurs. This method faces severe limits due to interannual differences in the meteorology and to differences in the local observation times at the satellites. However, this is expected to give a correct estimate of the error magnitude by taking into account the seasonal characteristics, including the astronomical variations of the incident solar fluxes. The differences in global and tropical (20°N, 20°S) means are generally less than 1 $W m^{-2}$ for both the LW and the SW monthly mean fluxes (Tables 2 and 3). For regional means, the standard deviation is around 10 $W m^{-2}$ for November 1998, December 1998, and January 1999. For February and March 1999, with better coverage, the error is smaller with a standard deviation of 3 $W m^{-2}$ in the LW and 4 $W m^{-2}$ in the SW. In sum-

TABLE 3. As in Table 2 but for the SW fluxes.

	Global means	Standard deviation	Tropical means
Nov 1994	+0.2	7.0	+0.0
Dec 1994	+0.2	10.3	+0.5
Jan 1995	+0.2	10.8	-0.3
Feb 1995	-0.1	4.5	+0.1
Mar 1994	-0.2	4.3	0.0

mary, the time sampling of ScaRaB-Resurs may have a relatively strong impact for the regional monthly mean fluxes but appears to have a rather weak impact (smaller than 1 W m^{-2}) for averages over the whole globe or over the tropical belt. These large-scale monthly mean values may therefore be compared to previous large-scale determinations based on ERBE, ScaRaB, and CERES scanner measurements.

2) LONG-TERM COMPARISONS

Interannual variations of the global monthly mean flux in the SW and the LW domain are relatively small with no obvious trends (Fig. 4). These interannual (and “interinstrumental”) variations hardly exceed 5 W m^{-2} for both spectral domains. The most striking feature is the shift of $2\text{--}3 \text{ W m}^{-2}$ in the LW outgoing radiation between the *NOAA-9* and the *NOAA-10* period of the ERBE program as already mentioned in Thomas et al. (1995). The measurements from ERBS/*NOAA-10* are in better agreement with the ScaRaB-Meteor measurements and give a net flux closer to equilibrium. The measurements from ScaRaB-Resurs gives a slightly larger outgoing LW compared to the other measurements. However, the shift does not exceed 1% and is thus within the error bar resulting from the calibration and processing uncertainties. In the SW spectral domain, the reflected flux difference is of the op-

posite sign but with a larger magnitude (up to 6% between ScaRaB-Meteor and ScaRaB-Resurs in Jan). This gives a net flux at the TOA that is in agreement with previous measurements by ERBE and ScaRaB-Meteor.

Considering the tropical zone (20°N , 20°S) only offers the opportunity to compare the interannual variations of ERBE, ScaRaB, and the CERES-TRMM dataset. This comparison is shown in Fig. 5, together with the continuous evolution of the National Oceanic and Atmospheric Administration (NOAA) outgoing longwave radiation (OLR; Liebmann and Smith 1996). For the period between 1994 and 1999, the NOAA OLR is underestimated by about 8.5 W m^{-2} compared to ScaRaB and CERES instruments (the point of Sep 1994 is suppressed from the figure since we have a problem here in our OLR time series). Apart from this constant underestimate of 8.5 W m^{-2} , there is a very good agreement between the NOAA OLR

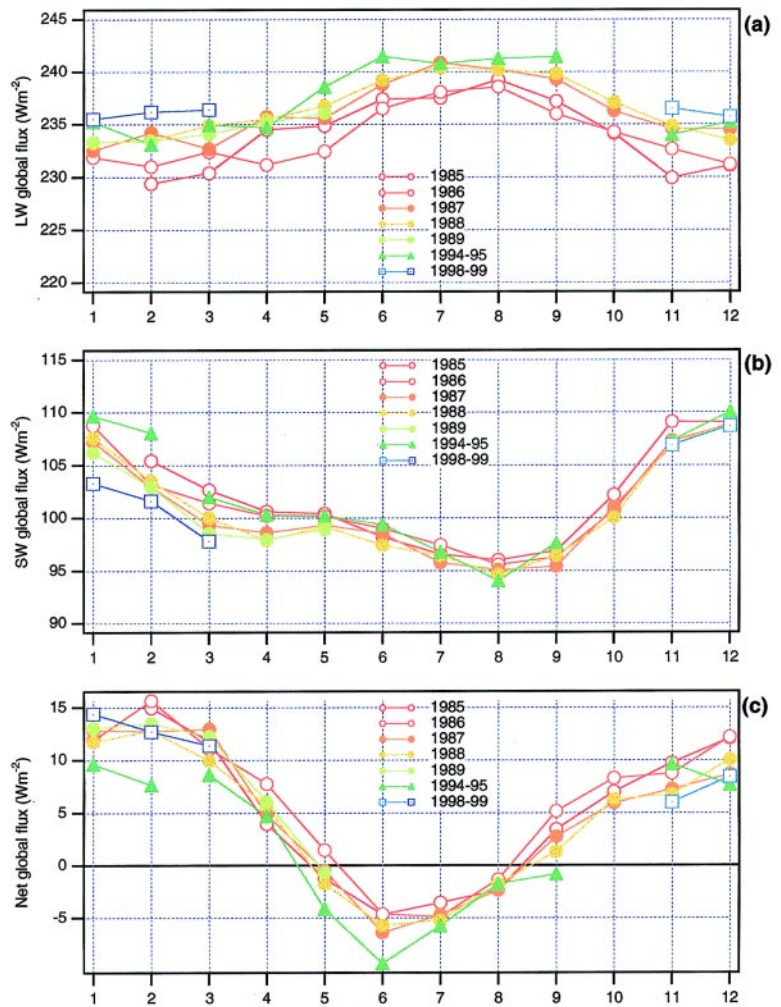


FIG. 4. Monthly mean global values for (a) the outgoing LW, (b) the reflected SW, and (c) the net fluxes for ERBE and ScaRaB experiments.

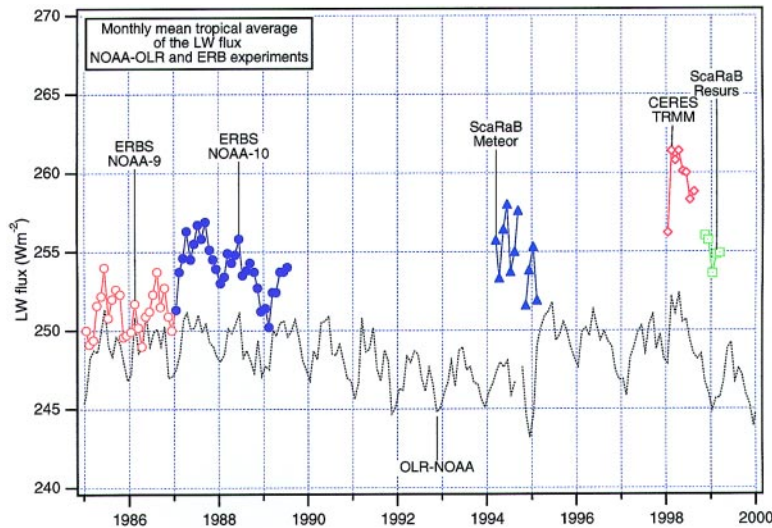


FIG. 5. Monthly mean tropical (20°N , 20°S) average of the outgoing LW fluxes for ERBE, CERES and ScaRaB experiments, and for the NOAA OLR time series.

time series, the ScaRaB measurements for the two flight models, and the CERES–TRMM measurements. In particular, the relatively large gap (of order 5 W m^{-2}) between the monthly tropical mean measured by CERES–TRMM and ScaRaB–Resurs is fully consistent with the variation of the NOAA OLR product. This difference is thus certainly a real geophysical signal of the transition from El Niño to La Niña between 1998 and 1999. However, compared to ERBE measurements, the NOAA OLR is underestimated by about 4 W m^{-2} (instead of 8.5 W m^{-2} for ScaRaB and CERES–TRMM). A similar comparison, done using the ERBE nonscanner wide-field-of-view dataset extending from 1985 through 1998, shows good consistency between the continuous ERBS dataset and the corresponding ERBE, ScaRaB–Meteor, and CERES–TRMM scanner data products (Wielicki et al. 1999). The fact that, after a period of relative consistency with ERBE products between 1985 and 1989, the difference between the NOAA OLR and the broadband

products showed an increase in following years (see Fig. 5) may be related in part to changes in equatorial crossing time already discussed by Waliser and Zhou (1997) and by Lucas et al. (2001). This is however more likely due to absolute calibration and narrow- to broadband problems and illustrates the difficulty resulting from the use of multiplatform radiometer to estimate precisely (better than 5 W m^{-2}) long-term variations of the outgoing LW fluxes. Note also that the difference between the NOAA-9 and NOAA-10 period of ERBE appears to have no equivalent in the NOAA OLR time series, confirming a likely calibration and processing problem in the determination of the LW radiance.

3) REGIONAL MEAN FLUXES

The mean regional ($2.5^{\circ} \times 2.5^{\circ}$) fluxes for winter 1999 (Jan, Feb, and Mar) are shown in Fig. 6, together

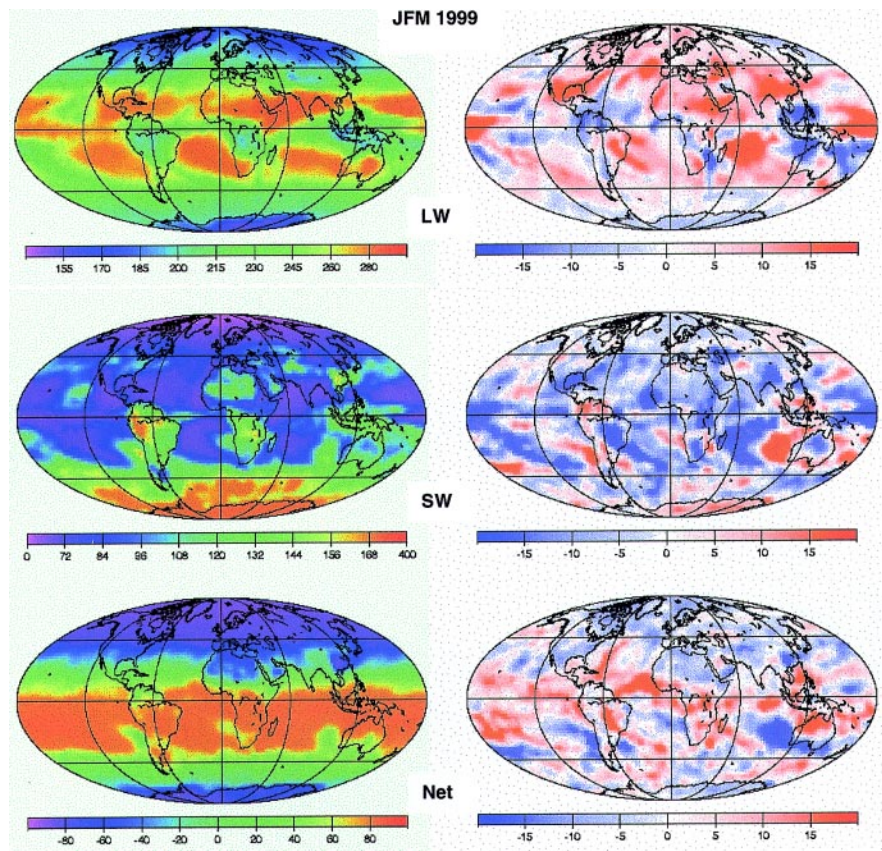


FIG. 6. (left) Regional fluxes (average for Jan, Feb, and Mar 1999) and (right) flux anomaly relative to the average for ERBE and ScaRaB–Meteor for the same months of the period 1985–89 and 1994–95. (top) LW, (middle) SW, and (bottom) net fluxes (W m^{-2}).

with the anomaly in regard to an average over the ERBE scanner (1984–89) and the ScaRaB-Meteor (1994–95) period for the same months. The average over these three months well summarizes the ScaRaB-Resurs results and decreases the error due to the lack of data. The SW, LW, and net CRF parameters for the same period are shown in Fig. 7.

In the LW, the weak global positive anomaly suggested in Fig. 4 appears to result from anomalies greater than $+10 \text{ W m}^{-2}$ distributed over all the globe (Fig. 6) with maximum values over the tropical belt and in particular over the Indian Ocean and the western Pacific. Strong negative anomalies correspond mainly to deep convective cloudiness in the equatorial zone, with maximum values over North Australia and Indonesia. The largest anomaly thus corresponds to an increased convective activity over the Indonesian region and less convective activity (or more subsidence) that increases the LW flux over the Indian Ocean, the western Pacific, and China. This feature, also manifest on the LW CRF map (Fig. 7) is related to the La Niña event of winter 1999. For regions around Indonesia, this anomaly is associated with positive and negative radiative perturbations in the LW of up to 20 W m^{-2} .

In the SW, the pattern is reversed but very similar. The maximum positive anomaly (i.e., more reflected SW in 1999) is located west of Australia. This suggests a larger amount of low-level boundary layer cloud (small impact in the LW) over the eastern part of the Indian Ocean associated with a smaller amount over the western part. A similar pattern is also evident in the South Atlantic Ocean west of Namibia and over the eastern Pacific west of Chile. This may correspond to a reinforcement of the SW cooling effect of cloud on the eastern edge and to an increased SW absorption on the western edge of the Southern Ocean during winter 1999. Part of this anomaly can however also be attributed to the limited temporal sampling provided by the Resurs satellite (1015 LST sun-synchronous) compared to the precessing ERBS and Meteor platforms. These stratocumulus clouds have a maximum coverage at sunrise and a minimum at sunset, giving an overestimate of the albedo for measurements from a sun-synchronous morning satellite. This is a known problem and different solutions to improve the diurnal correction models have already been proposed in Haeffelin et al. (1999) and in Standfuss et al. (2001). For the net flux and the net CRF there

also is a net cooling anomaly at the eastern edges of the Indian, the Pacific, and the Atlantic Oceans. As reported in earlier studies (Harrison et al. 1990), the CRF parameter is smaller over the equatorial region, due to near cancellation between the SW cooling and the relatively strong LW warming of the high (cold) convective cloud tops. As for the LW and the SW TOA fluxes, the anomaly in the net flux (Fig. 6) is very similar to the anomaly in the net CRF (Fig. 7). This illustrates the paramount importance of the cloudiness in the interannual variations of radiation balance at regional scales.

4. Conclusions

Broadband radiance measurements made by the ScaRaB-Resurs instrument exhibit strong

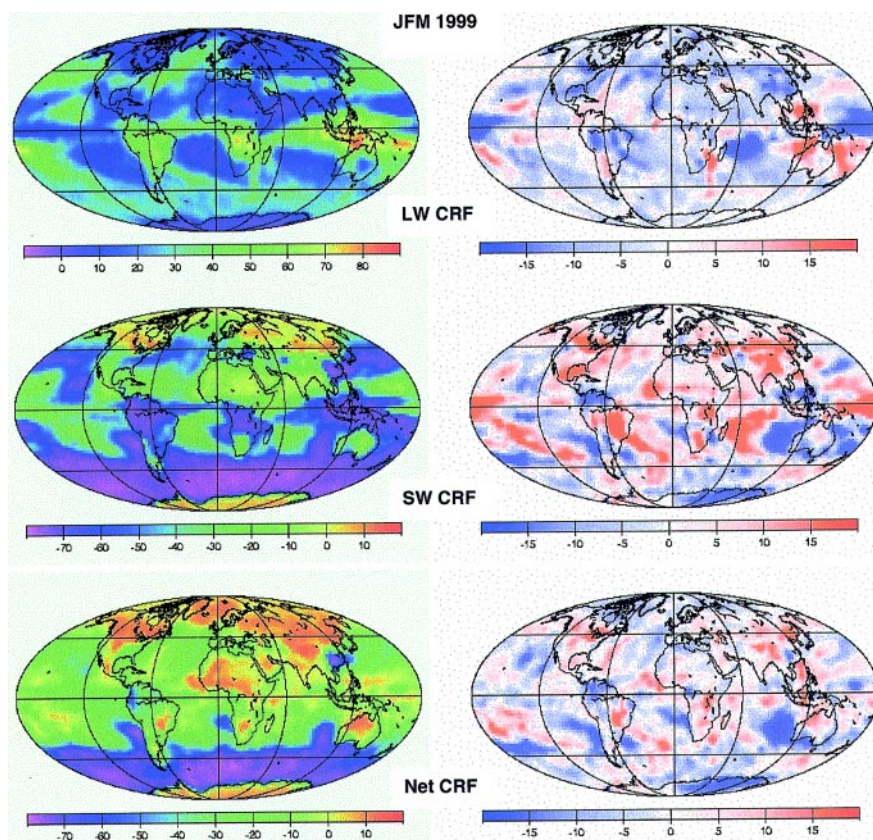


FIG. 7. As in Fig. 6 but for the CRF parameter in W m^{-2} .

consistency with earlier ERB measurements, while at the same time revealing significant regional and zonal anomalies specific to the 1998/99 El Niño–La Niña transition. There is excellent agreement with the CERES–TRMM instrument, as demonstrated by direct comparison of simultaneous collocated codirectional broadband radiance measurements. The highly accurate ScaRaB–Resurs broadband radiances are therefore valuable for case studies (Kozoderov and Golovko 1999; Golovko and Kozoderov 2000) or in complement to field experiments such as the Indian Ocean Experiment (Crutzen and Ramanathan 2001; Coakley et al. 2001) in a period with no other ERB scanner in operation. Despite the relatively large amount of missing data, this dataset still makes it possible to quantify the regional radiative anomalies in the winter of 1999, particularly in regard to the La Niña phase of the Southern Oscillation.

This second experiment concludes the cooperative ScaRaB program of France, Russia, and Germany. The major originality of this program, apart from the link of Russian (initially Soviet), French, and German space activities in earth observation, was the instrumental design that gave very reliable radiance measurements both in broad and narrow bands. The availability of well-registered narrow- and broadband channels is an original feature of the ScaRaB instrument that gives unique information valuable for further scientific analyses. In the SW spectral domain such an analysis (Duvel et al. 2000) shows that, with correct conversion coefficients and with an appropriate processing, SW fluxes estimated from VIS measurements may have biases smaller than 2% for either instantaneous or monthly mean regional fluxes. The standard deviation of the error in these monthly mean regional SW fluxes may be as small as 4%, a value comparable to the expected temporal sampling error made by two polar orbiting satellites. However, calibration and processing certainly remain the most important problems for the determination of the ERB parameter using only narrowband radiometers. Further analysis of the ScaRaB measurements is still necessary to complete the error budget resulting from the use of narrowband channels of operational meteorological satellites to monitor the earth radiation budget and its modulation by cloudiness.

Acknowledgments. We thank Francis Sirou (the ScaRaB–Resurs instrument project chief at LMD), Bernard Briot, Alain Pellegrin, and Bernard Gillet at LMD, as well as the other engineers and technicians at Palaiseau (LMD), Orsay (IAS), Toulouse (CNES), Moscow (NITsIPR), Munich (Sensorlab), and at the

ground calibration site at Odeillo for their enthusiasm and their invaluable participation in the ScaRaB project. Data access and other information may be found online at scarab.cnes.fr and at lmdx.polytechnique.fr/~ScaRaB.

References

- Barkstrom, B. R., E. F. Harrison, G. L. Smith, R. Green, J. Kibler, R. D. Cess, and the ERBE Science Team, 1989: Earth Radiation Budget Experiment (ERBE) archival and April 1985 results. *Bull. Amer. Meteor. Soc.*, **70**, 1254–1262.
- Bony, S., and J.-Ph. Duvel, 1994: Influence of the vertical structure of the atmosphere on the seasonal variation of precipitable water and greenhouse effect. *J. Geophys. Res.*, **99**, 12 963–12 980.
- , —, and H. Le Treut, 1995: Observed dependence of the water vapor and clear-sky greenhouse effect on sea surface temperature: Comparison with climate warming experiments. *Climate Dyn.*, **11**, 307–320.
- Briand, V., C. J. Stubenrauch, W. B. Rossow, A. Walker, and R. Holz, 1997: Scene identification for ScaRaB data: the ISCCP approach. *Satellite Remote Sensing of Clouds and the Atmosphere*, J. D. Haigh, Ed., SPIE, 242–252.
- Cess, R. D., and Coauthors, 1990: Intercomparison and interpretation of climate feedback processes in 19 atmospheric general circulation models. *J. Geophys. Res.*, **95**, 16 601–16 615.
- Charlock, T. P., and V. Ramanathan, 1985: The albedo field and cloud radiative forcing produced by a general circulation model with internally generated cloud optics. *J. Atmos. Sci.*, **42**, 1408–1429.
- Coakley, J. A., and D. G. Baldwin, 1984: Toward the objective analysis of clouds from satellite imagery data. *J. Climate Appl. Meteor.*, **23**, 1065–1099.
- , and Coauthors, 2001: General overview of INDOEX. *J. Geophys. Res.*, in press.
- Crutzen, P. J., and V. Ramanathan, 2001: Indian Ocean Experiment: Foreword to the special issue. *J. Geophys. Res.*, in press.
- Dinguirard, M., J. Mueller, F. Sirou, and T. Tremas, 1998: Comparison of ScaRaB ground calibration in the short wave and long wave domains. *Metrologia*, **35**, 597–601.
- Duvel, J.-Ph., and P. Raberanto, 2000: A geophysical cross-calibration approach for broadband channels: Application to the ScaRaB experiment. *J. Atmos. Oceanic Technol.*, **17**, 1609–1617.
- , S. Bony, H. Le Treut, and participating AMIP modeling groups, 1997: Clear-sky greenhouse effect sensitivity to sea surface temperature changes: An evaluation of AMIP simulations. *Climate Dyn.*, **13**, 259–273.
- , S. Bouffiès-Cloch , and M. Viollier, 2000: Determination of shortwave earth reflectances from visible radiance measurements: Error estimate using ScaRaB data. *J. Appl. Meteor.*, **39**, 957–970.
- Fouquart, Y., J. C. Buriez, M. Herman, and R. S. Kandel, 1990: The influence of clouds on radiation: a climate-modeling perspective. *Rev. Geophys.*, **28**, 145–166.
- Golovko V. A., and V. V. Kozoderov, 2000: Earth radiation budget: New applications to study natural hazards from space. *Russ. J. Remote Sens.*, **1**, 29–41.

- Haeffelin, M., R. Kandel, and C. Stubenrauch, 1999: Improved diurnal interpolation of reflected broadband observations using ISCCP data. *J. Atmos. Oceanic Technol.*, **16**, 38–54.
- , B. Wielicki, J.-Ph. Duvel, K. Priestley, and M. Viollier, 2001: Intercalibration of CERES and ScaRaB Earth radiation budget datasets using temporally and spatially collocated radiance measurements. *Geophys. Res. Lett.*, **28**, 167–170.
- Harrison, E. F., P. Minnis, B. R. Barkstrom, V. Ramanathan, R. D. Cess, and G. G. Gibson, 1990: Seasonal variation of cloud radiative forcing derived from the Earth Radiation Budget Experiment. *J. Geophys. Res.*, **95**, 18 687–18 703.
- Hartmann, D. L., V. Ramanathan, A. Berroir, and G. E. Hunt, 1986: Earth radiation budget data and climate research. *Rev. Geophys.*, **24**, 439–468.
- House, F. B., A. Gruber, G. E. Hunt, and A. T. Mecherikunnel, 1986: History of satellite missions and measurements of the Earth Radiation Budget. *Rev. Geophys.*, **24**, 357–377.
- Jacobowitz, H., H. V. Soule, H. L. Kyle, F. B. House, and the Nimbus-7 ERB Experiment Team, 1984: The Earth Radiation Budget (ERB) experiment: An overview. *J. Geophys. Res.*, **89**, 5021–5038.
- Kandel, R. S., 1990: Satellite observations of the Earth radiation budget and clouds. *Space Sci. Rev.*, **52**, 1–32.
- , and Coauthors, 1998: The ScaRaB Earth Radiation Budget Dataset. *Bull. Amer. Meteor. Soc.*, **79**, 765–783.
- Kozoderov, V. V., and V. A. Golovko, 1999: Interpretation and analysis of the earth radiation budget components from space. *Proc. Third Int. Scientific Conf. on the Global Energy and Water Cycle*, Beijing, China, CMO, 173–174.
- Levitus, S., J. I. Antonov, T. P. Boyer, and C. Stephens, 2000: Warming of the world ocean. *Science*, **287**, 2225–2229.
- Li, Z., and A. Trishchenko, 1999: A study toward an improved understanding of the relationship between visible and shortwave albedo measurements. *J. Atmos. Oceanic Technol.*, **16**, 347–360.
- Liebmann, B., and C. A. Smith, 1996: Description of a complete (interpolated) outgoing longwave radiation dataset. *Bull. Amer. Meteor. Soc.*, **77**, 1275–1277.
- Lucas, L. E., D. E. Waliser, P. Xie, J. E. Janowiak, and B. Liebman, 2001: Estimating the satellite equatorial crossing time biases in the daily, global outgoing longwave radiation dataset. *J. Climate*, in press.
- Monge, J. L., R. S. Kandel, L. A. Pakhomov, and V. I. Adasko, 1991: ScaRaB earth radiation budget scanning radiometer. *Metrologia*, **28**, 261–284.
- Mueller, J., R. Stuhlmann, E. Raschke, J. L. Monge, R. Kandel, P. Burkert, and L. A. Pakhomov, 1993: Solar ground calibration of ScaRaB preliminary results. *Passive Infrared Remote Sensing of Clouds and the Atmosphere*, D. K. Lynch, Ed., SPIE, 129–139.
- , —, R. Becker, E. Raschke, J. L. Monge, and P. Burkert, 1996: Ground-based calibration facility for the Scanner for Radiation Budget instrument in the solar spectral domain. *Metrologia*, **32**, 657–660.
- , —, —, —, and Coauthors, 1997: Ground Characterization of the Scanner for Radiation Budget (ScaRaB) Flight Model 1. *J. Atmos. Oceanic Technol.*, **14**, 802–813.
- Ramanathan, V., R. D. Cess, E. F. Harrison, P. Minnis, B. R. Barkstrom, E. Ahmad, and D. Hartmann, 1989: Cloud-radiative forcing and climate: Results from the Earth Radiation Budget Experiment. *Science*, **243**, 57–63.
- Raschke, E., T. H. Vonder Haar, W. R. Bandeen, and M. Pasternak, 1973: The annual radiation balance of the earth–atmosphere system during 1969–1970 from Nimbus-3 measurements. *J. Atmos. Sci.*, **30**, 341–364.
- Raval, A., and V. Ramanathan, 1989: Observational determination of the greenhouse effect. *Nature*, **342**, 758–761.
- Standfuss, C., M. Viollier, R. S. Kandel, and J. P. Duvel, 2001: Regional diurnal albedo climatology and diurnal time extrapolation of reflected solar flux observations: Application to the ScaRaB record. *J. Climate*, **14**, 1129–1146.
- Stephens, G. L., and T. J. Greenwald, 1991a: The Earth’s radiation budget and its relation to atmospheric hydrology 1. Observations of the clear sky greenhouse effect. *J. Geophys. Res.*, **96**, 15 311–15 324.
- , and —, 1991b: The Earth’s radiation budget and its relation to atmospheric hydrology 2. Observations of cloud effect. *J. Geophys. Res.*, **96**, 15 325–15 340.
- , G. G. Campbell, and T. H. Vonder Haar, 1981: Earth radiation budgets measurements from satellites and their interpretation for climate modeling and studies. *J. Geophys. Res.*, **86**, 9739–9760.
- Stowe, L. L., Ed., 1988: Report of the earth radiation budget requirements review—1987. NOAA Tech. Rep. NESDIS-41, 103 pp.
- Stubenrauch, C. J., J.-Ph. Duvel, and R. S. Kandel, 1993: Determination of longwave anisotropic emission factors from combined broad- and narrow-band radiance measurements. *J. Appl. Meteor.*, **32**, 848–856.
- Thomas, D., J.-Ph. Duvel, and R. S. Kandel, 1995: Diurnal bias in calibration of broad-band radiance measurements from space. *IEEE Trans. Geosci. Remote Sens.*, **33**, 670–683.
- Viollier, M., R. Kandel, and P. Raberanto, 1995: Inversion and space-time averaging algorithms for ScaRaB (Scanner for Earth Radiation Budget)—Comparison with ERBE. *Ann. Geophys.*, **13**, 959–968.
- Waliser, D. E., and W. Zhou, 1997: Removing satellite equatorial crossing time biases from the OLR and HRC datasets. *J. Climate*, **10**, 2125–2146.
- Wielicki, B. A., B. R. Barkstrom, E. F. Harrison, R. B. Lee III, G. L. Smith, and J. E. Cooper, 1996: Clouds and the Earth’s Radiant Energy System (CERES): An Earth Observing System experiment. *Bull. Amer. Meteor. Soc.*, **77**, 853–868.
- , T. Wong, D. F. Young, B. R. Barkstrom, R. B. Lee, and M. Haeffelin, 1999: Differences between ERBE and CERES tropical mean fluxes: ENSO, climate or calibration? Preprints, *10th Conf. on Atmospheric Radiation*, Madison, WI, Amer. Meteor. Soc., 48–51.